HNPS Advances in Nuclear Physics

Vol 28 (2021)

HNPS2021

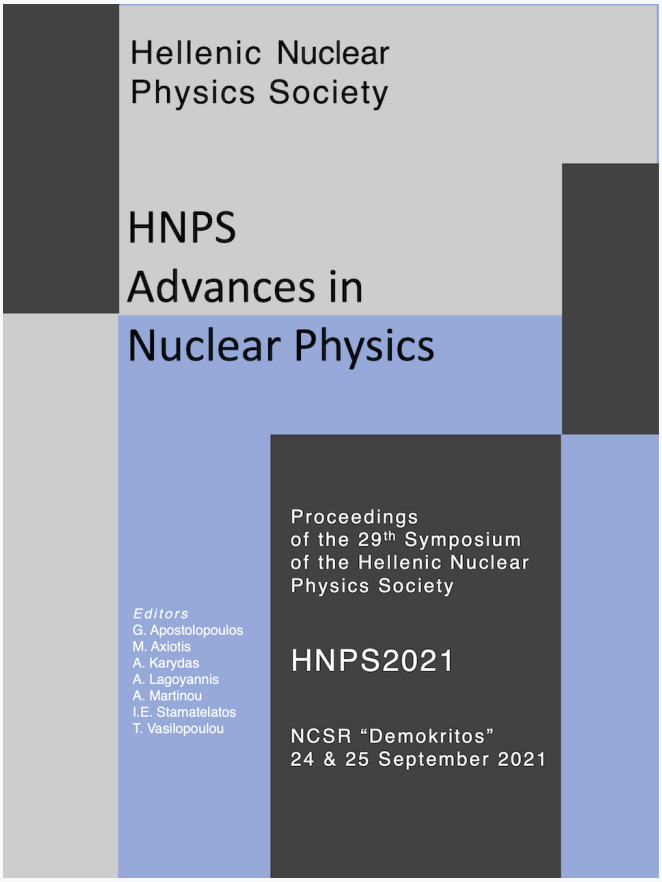

Study of Multinucleon Transfer Mechanisms in 86Kr-Induced Peripheral Reactions at 15 and 25 MeV/nucleon

Olga Fasoula, George Souliotis, Stergios Koulouris, Konstantina Palli, Martin Veselsky, Sherry Yenello, Aldo Bonasera

doi: 10.12681/hnps.3572

To cite this article:

Fasoula, O., Souliotis, G., Koulouris, S., Palli, K., Veselsky, M., Yenello, S., & Bonasera, A. (2022). Study of Multinucleon Transfer Mechanisms in 86Kr-Induced Peripheral Reactions at 15 and 25 MeV/nucleon. *HNPS Advances in Nuclear Physics*, *28*, 47–53. https://doi.org/10.12681/hnps.3572

Study of Multinucleon Transfer Mechanisms in ^{86}Kr-Induced Peripheral Reactions at 15 and 25 MeV/nucleon

O. Fasoula[1], G.A. Souliotis[1,*], S. Koulouris[1], K. Palli[1], M. Veselsky[2], S.J. Yenello[3], A. Bonasera[3]

[1] *Laboratory of Physical Chemistry, Department of Chemistry, National and Kapodistrian University of Athens*
[2] *Institute of Experimental and Applied Physics, Czech Technical University, Prague, Czech Republic*
[3] *Cyclotron Institute, Texas A&M University, College Station, Texas, USA*

Abstract This paper presents our recent studies of the multinucleon transfer in peripheral collisions in reactions near the Fermi regime. Specifically, the reactions of an ^{86}Kr beam at 15 MeV/nucleon with targets of ^{124}Sn ,^{112}Sn, ^{64}Ni, and ^{58}Ni and reactions of an ^{86}Kr beam at 25 MeV/nucleon with targets of ^{124}Sn and ^{112}Sn. The experimental data were obtained from the previous work of our group with the MARS spectrometer at the Cyclotron Institute of Texas A&M University. Our current focus is the thorough study of the experimental mass and momentum distributions of the projectile-like fragments. The momentum distributions are characterized by a narrow quasi-elastic peak and a broader deep-inelastic peak. We employed two-body kinematics to characterize the excitation energies of these reactions. We also compared the data with model calculations. The dynamical stage is described with either the Deep-Inelastic Transfer Model (DIT), or with the microscopic Constrained Molecular Dynamics model (CoMD). The de-excitation of the hot projectile-like fragments is performed with the Gemini model. Studying these reactions will provide us with a better understanding of how the energy of the beam and the different targets affect the mechanism of the multinucleon transfer reactions. With the recent work, our continued efforts in the study of peripheral reactions in the Fermi energy regime delineate new opportunities to elucidate the reaction mechanism(s) of rare isotope production and may effectively contribute to the study of unexplored regions of the nuclear chart toward the r-process and the neutron drip line.

Keywords multinucleon transfer, momentum distribution, Fermi energy regime, neutron rich isotopes, deep inelastic transfer

INTRODUCTION

One of the core interests of the nuclear physics community is the exploration of the nuclear landscape toward the neutron rich nuclei of the astrophysical r-process and the neutron dripline [1-8]. To experimentally reach these extremely neutron rich nuclei, it is necessary to pick up neutrons from the target. This possibility is offered by multinucleon exchange reactions at the Fermi energy regime (15-35 MeV/nucleon) [9-11], which is the focus of our group [12-14]. The reactions of this region combine the advantages of high (fragmentation) and low energy (near the Coulomb barrier) reactions where the projectile can interact with a neutron rich target resulting in fragments with high neutron excess. To this end, in this work we present the systematic study of experimental data from reactions with an ^{86}Kr beam at 15 MeV/nucleon with targets of ^{124}Sn, ^{112}Sn, ^{64}Ni and ^{58}Ni and reactions of an ^{86}Kr beam at 25 MeV/nucleon with targets of ^{124}Sn and ^{112}Sn. The experimental data were obtained in previous works of our group. Both the 15 MeV/nucleon [11] and the 25 MeV/nucleon data [10] were obtained with the Momentum Achromat Recoil Separator (MARS) [11] at the Cyclotron Institute of Texas A&M University. For the present systematic analysis of the experimental data, the momentum distributions of the projectile-like fragments were recently extracted from the original data [11]. We also present some preliminary calculations with two models: The Deep Inelastic Transfer (DIT) model [15] and the Constrained Molecular Dynamics (CoMD) model [16-18] both followed by the Gemini

* Corresponding author: soulioti@chem.uoa.gr

model [19,20] for the de-excitation of the primary projectile-like fragments.

EXPERIMENTAL DISTRIBUTIONS

The first part of this paper focuses on the experimental distributions of projectile-like fragments from reactions of an ^{86}Kr beam at 15 MeV/nucleon with targets of ^{64}Ni, ^{58}Ni, ^{112}Sn and ^{124}Sn and reactions with an ^{86}Kr beam at 25 MeV/nucleon with targets of ^{124}Sn and ^{112}Sn.

Mass distributions: 15 MeV/nucleon ^{86}Kr + ^{64}Ni/^{58}Ni

To begin with, in Fig. 1 we present the experimental mass distributions of projectile-like fragments with Z=30-37 from the reaction 15 MeV/nucleon ^{86}Kr + ^{64}Ni/^{58}Ni. These results have been published by our group in [11].

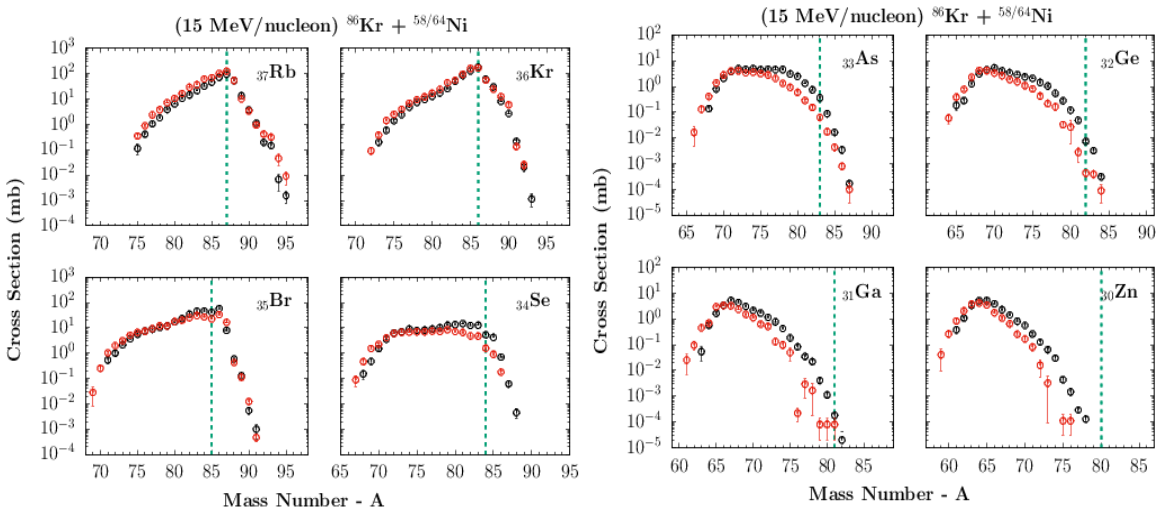

Fig. 1. *Experimental mass distribution of projectile-like fragments from reactions 15 MeV/nucleon ^{86}Kr + ^{64}Ni (black dots) and 15 MeV/nucleon ^{86}Kr + ^{58}Ni (red dots). Green dashed lines indicate the beginning of neutron pickup.*

Both sets of data have overall the same shape, with those of ^{64}Ni being higher than ^{58}Ni especially in the neutron rich region. It is also noteworthy that production of neutron rich isotopes is observed especially in masses near the projectile. Namely, for Kr the pickup of up to 7 neutrons is observed and for Br, Se and As the pickup of up to 4 neutrons is observed.

Mass distributions: 15 MeV/nucleon ^{86}Kr + ^{124}Sn/^{112}Sn

Furthermore, in Fig. 2 we present the experimental mass distributions of projectile-like fragments in the same atomic number region and same ^{86}Kr beam but with targets of ^{124}Sn and ^{112}Sn [11]. Black dots represent the ^{124}Sn data and red dots represent the ^{112}Sn data.

As in the previous reactions, both data sets show the same overall shape, with the neutron rich target of ^{124}Sn yielding higher cross sections than the neutron deficient target of ^{112}Sn, especially in the neutron rich region. Very neutron rich isotopes can be produced with these reactions as well. Specifically, for Krypton and Selenium the pickup of up to 6 neutrons is observed and for Bromine and Germanium the pickup of up to 4 neutrons is observed.

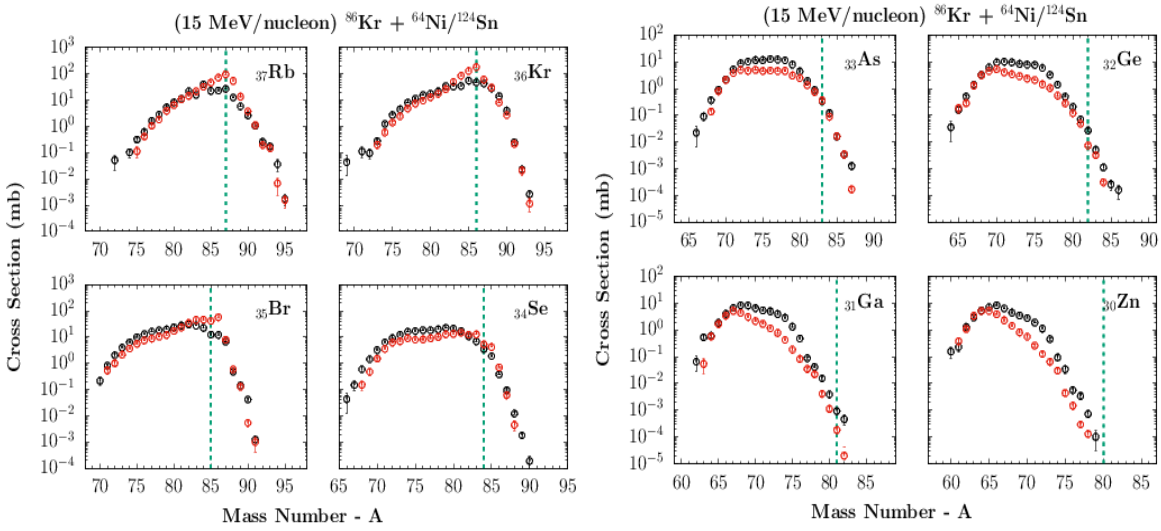

Fig. 2. *Experimental mass distribution of projectile-like fragments from reactions 15 MeV/nucleon ^{86}Kr + ^{124}Sn (black dots) and 15 MeV/nucleon ^{86}Kr + ^{112}Sn (red dots). Green dashed lines indicate the beginning of neutron pickup.*

Mass distributions: 15/25 MeV/nucleon ^{86}Kr + ^{124}Sn

In Fig. 3 we present a comparison of the two reactions with a target of ^{124}Sn and the ^{86}Kr beams at the two different energies (15 and 25 MeV/nucleon) [10,11]. Black dots represent the 15 MeV/nucleon data and red dots represent the 25 MeV/nucleon data.

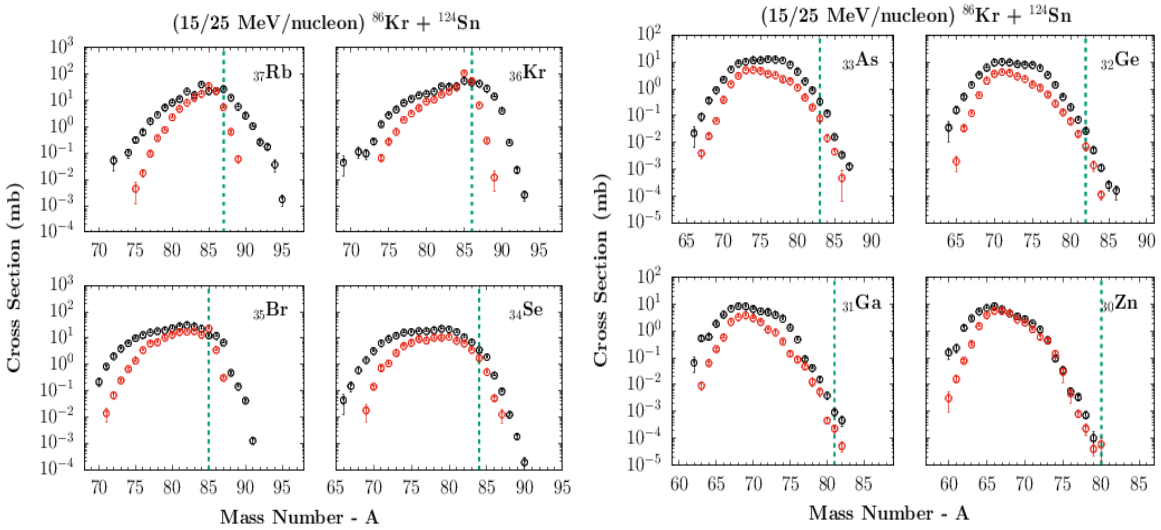

Fig. 3. *Experimental mass distribution of projectile-like fragments from reactions 15 MeV/nucleon ^{86}Kr + ^{124}Sn (black dots) and 25 MeV/nucleon ^{86}Kr + ^{124}Sn (red dots). Green dashed lines indicate the beginning of neutron pickup.*

This comparison is one of the ways we can use to assess how the energy of the beam affects the production of isotopes. The 25 MeV/nucleon data seem to have narrower distributions than the 15 MeV/nucleon data, a trend that persists to various degrees throughout this mass region. Especially in the right part (the neutron rich side) of the distributions, the 15 MeV/nucleon data yield more neutron rich isotopes hinting that a beam with lower energy may be more favorable in the pursuit of neutron rich nuclei.

Momentum distributions - Neutron Pickup Channels: 15 MeV/nucleon ^{86}Kr + ^{124}Sn

A new part of our work is the study of the momentum distributions of projectile fragments. In Fig. 4 we present the reaction of ^{86}Kr at 15 MeV/nucleon with a target of ^{124}Sn, specifically the channels representing the pickup of 1 to 4 neutrons. These data have been recently extracted from the original experimental data [11]. Each panel represents a specific isotope and the corresponding momentum per nucleon and differential cross sections. Black dots and lines represent the ^{124}Sn data and red dots and lines represent the ^{112}Sn data. Generally, both distributions are characterized by two main regions. A sharper peak that corresponds to quasi-elastic events with low total kinetic energy loss and a broader region at lower values of momentum per nucleon that corresponds to more dissipative events with larger total kinetic energy loss. This points to the fact that the nuclei that reach the spectrometer are not solely products of quasi-elastic scattering and come from multinucleon transfer reactions where the primary excited fragments were finally de-excited via nucleon evaporation. The numbers on top of the peaks are the total excitation energies (in MeV) obtained by binary kinematics calculations.

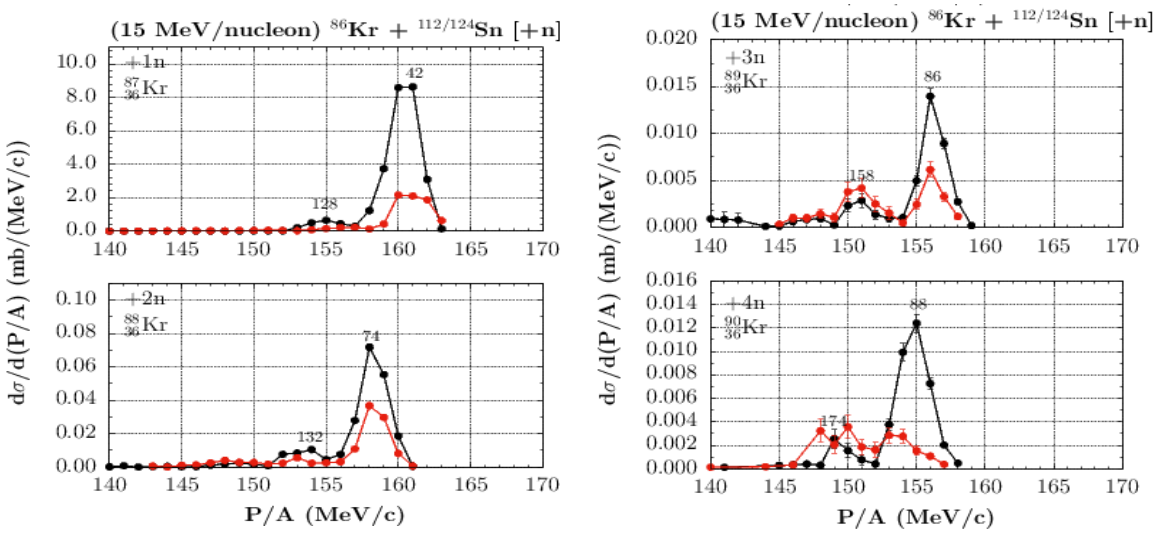

Fig. 4. *Experimental momentum distribution of projectile-like fragments from reactions 15 MeV/nucleon ^{86}Kr + ^{124}Sn (black dots) and 15 MeV/nucleon ^{86}Kr + ^{112}Sn (red dots).*

For all Krypton isotopes the projectile-like fragments from the reaction with ^{124}Sn have larger cross sections than those of ^{112}Sn as it was observed in the mass distributions before. The detailed study of the momentum distributions is a new study path for our group which may shed light to the reaction mechanisms in the Fermi energy regime.

THEORETICAL MODELS

The mass distributions were compared with model calculations employing a two-stage approach. The dynamic part of the reactions was simulated either with the Deep Inelastic Transfer model or the Constrained Molecular Dynamics model. The de-excitation of the hot projectile-like fragments was performed by the Gemini model.

The DIT model [15] is a phenomenological model used in peripheral collisions and it simulates the stochastic exchange of nucleons via a ‘window’ between the projectile and the target. The CoMD model [16-18] is a microscopic, semiclassical model based on quantum dynamics. The nucleons are considered as Gaussian wave packets, and the interactions take place via a phenomenological effective

potential. The fermionic nature of the system is introduced by the Pauli principle through proper restrictions in the phase space. In both models, successive events are simulated through Monte Carlo implementation. The Gemini [19,20] model, used for de-excitation of the primary nuclei after the interaction, is a binary de-excitation model.

CALCULATIONS

Mass distributions: 15 MeV/nucleon ^{86}Kr + ^{124}Sn

In Fig. 5 we present the comparison of calculations with the DIT (yellow lines) and CoMD (red lines) models (both followed by the Gemini model) with experimental data on the reaction of ^{86}Kr at 15 MeV/nucleon with a target of ^{124}Sn. The general layout is the same as in the experimental mass distribution presented earlier. Dashed lines represent the primary hot projectile-like fragments and solid lines represent fragments after the de-excitation.

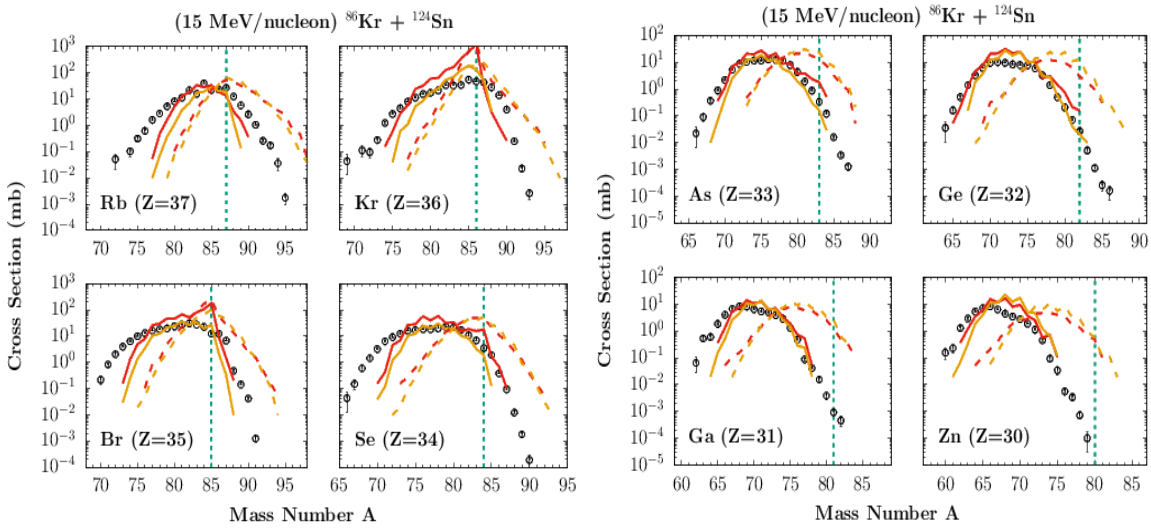

Fig. 5. *Comparison of calculations with experimental mass distribution of projectile-like fragments from the reaction of 15 MeV/nucleon ^{86}Kr + ^{124}Sn. Solid red lines: COMD/GEM for the de-excited projectile-like fragments. Dashed red lines: COMD/GEM for the primary projectile-like fragments. Solid yellow lines: DIT/GEM for the de-excited projectile-like fragments. Dashed yellow lines: DIT/GEM for the primary projectile-like fragments. Green dashed lines indicate the beginning of neutron pickup.*

It is noteworthy that both DIT and CoMD calculations give the same shape for the primary fragments. Two models with different parameters and approaches in describing the nuclear interactions yield the same overall results. This gives us the confidence that these models could adequately describe the dynamical stage of these heavy-ion reactions.

This, however, changes in some instances after the de-excitation. Specifically, in the neutron rich region, the DIT/GEM calculations are lower than the CoMD/GEM calculations. This can be explained by the fact that the DIT calculations seem to have larger values of excitation energies, a fact that is apparent in all distributions and is previously reported in the literature. To correct this tendency and adequately describe the experimental distributions, preliminary calculations indicate that a scaling factor of 0.7-0.8 should be employed. Generally, both calculations after the de-excitation appear to agree with the experimental results especially in mass ranges near the projectile (Z=34-32).

Excitation Energies: 15 MeV/nucleon ^{86}Kr + ^{124}Sn

To elucidate the role of the excitation energies of the nuclei that are produced, in Fig. 6 we present the mean excitation energy for each isotope in the same range of atomic numbers as in the mass distributions.

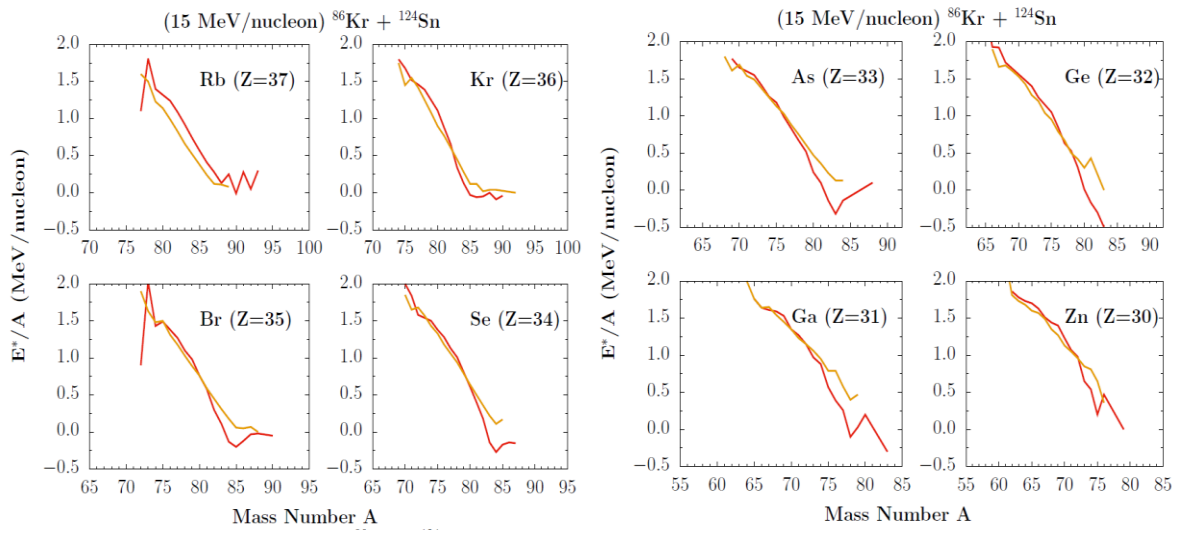

Fig. 6. *Total excitation energy per nucleon of projectile-like fragments from the reaction of 15 MeV/nucleon ^{86}Kr + ^{124}Sn. Solid red lines: COMD/GEM for the de-excited projectile-like fragments. Solid yellow lines: DIT/GEM for the de-excited projectile-like fragments.*

As expected, the excitation energies of the DIT calculations are higher than the CoMD calculations mostly on the neutron rich side.

The negative excitation energies in the CoMD model indicate a 'weakness' in these calculations. For some events of very peripheral collisions the excited states of the projectiles have binding energies lower than the ground state resulting in the negative values of the excitation energies. This is something that we are currently working to improve.

CONCLUSIONS

In this work, we presented a systematic study of experimental distributions on reactions with an ^{86}Kr beam at 15 and 25 MeV/nucleon with various targets (^{124}Sn, ^{112}Sn, ^{64}Ni. ^{58}Ni). The mass distributions and the recently extracted momentum distributions of the projectile-like fragments indicate the production of very neutron rich isotopes. We also performed calculations with the DIT and CoMD models with promising results in describing these reactions, a fact supported by the agreement of both models on the yield calculations of the primary hot projectile-like fragments.

We plan to pursue the systematic analysis of the experimental data in mass and momentum distributions, to perform more thorough kinematic analysis on the momentum distributions and attempt to reconstruct the quasi-projectile. Furthermore, we also plan to perform calculations with theoretical models and improve their parameters in order to effectively describe nuclear reactions that result in the production of neutron rich nuclei. These endeavors are important as we may gain information about the reaction mechanisms in energies below the Fermi energy regime and on the production of very neutron rich isotopes.

References

[1] Q. Z. Chai, Y. Qiang, J. C. Pei, Phys. Rev. C 105, 034315 (2022)
[2] F. Nowacki, A. Obertelli, A. Poves, Prog. Part. Nucl. Phys. 120, 103866 (2021)
[3] J. J. Cowan et al., Rev. Mod. Phys. 93, 015002 (2021)
[4] C. J. Horowitz et al., J. Phys. G: Nucl. Part. Phys., 46, 083001 (2019)
[5] B. E. Margaret, et al. Rev. Mod. Phys. 29, 547 (1957)
[6] J. Erler et al, Nature 486, p.509 (2011)
[7] Y. Blumenfeld, T. Nilsson, P.V. Duppen, Phys. Scr. T 152, 014203 (2013)
[8] G. G. Adamian, N. V. Antonenko, A. Diaz-Torees, S. Heinz, Eur. Phys. J. A 56, p.47 (2020)
[9] G. A. Souliotis et al., Phys. Lett. B 543, p.163 (2002)
[10] G. A. Souliotis et al., Phys. Rev. Lett. 91, 022701 (2003)
[11] G. A. Souliotis et al., Phys. Rev. C 84, 064607 (2011)
[12] O. Fasoula, G. A. Souliotis et al., arXiv:2103.10688
[13] K. Palli, G. A. Soulioris, T. Depastas, I. Dimitropoulos, O. Fasoula, S. Koulouris et al., EPJ Web of Conferences 252, 07002 (2021)
[14] S. Koulouris, G.A. Souliotis, F. Cappuzzello, D. Carbone, A. Pakou et al., EPJ Web of Conferences 252, 07005 (2021)
[15] L. Tassan-Got and C. Stephan, Nucl. Phys. A 524, 121 (1991).
[16] M. Papa, T. Maruyama, A. Bonasera, Phys. Rev. C 64, 024612 (2001)
[17] M. Papa, G. Giuliani, and A. Bonasera, J. Comput. Phys. 208, 403 (2005)
[18] T. Depastas, G. A. Souliotis, K. Palli, A. Bonasera, H. Zheng, EPJ Web of Conferences 252, 07003 (2021)
[19] R. J. Charity et al., Nucl. Phys. A 483, p.371 (1988)
[20] R. J. Charity, Phys. Rev. C 58, 1073 (1998).